




The effect of *in situ* irradiation on the superconducting performance of REBa₂Cu₃O_{7-δ}-coated conductors

Will Iliffe, Kirk Adams, Nianhua Peng, Greg Brittles, Rod Bateman, Aidan Reilly, Chris Grovenor, and Susannah Speller* 

Impact statement

REBa₂Cu₃O_{7-δ} high-temperature superconductors are an enabling technology for plasma confinement magnets in compact commercial fusion power plants, owing to their ability to carry very high current densities when processed as quasi-single crystals in the form of coated conductors. In service in a fusion device, the magnet windings will be exposed to a flux of fast neutrons that will induce structural damage that will adversely affect the superconducting performance, but very little data are currently available on the effect of irradiation at the cryogenic temperatures relevant for superconducting magnets. Moreover, even room-temperature annealing substantially affects superconducting properties after irradiation, so to obtain key technical data for fusion magnet designers, it is important to measure these properties *in situ*, under irradiation. This work shows that for the first time, it is important to consider how energetic particles directly influence superconductivity during irradiation because we observe a reduction in zero-resistance current by a factor of as much as three when an ion beam is incident on the sample. Although neutrons will not interact with the material in the same way as charged ions, primary knock-on ions from neutron damage are expected to have a similar effect to the He⁺ ions used in our study.

Commercial fusion power plants will require strong magnetic fields that can only be achieved using state-of-the-art high-temperature superconductors in the form of REBa₂Cu₃O_{7-δ}-coated conductors. In operation in a fusion machine, the magnet windings will be exposed to fast neutrons that are known to adversely affect the superconducting properties of REBa₂Cu₃O_{7-δ} compounds. However, very little is known about how these materials will perform when they are irradiated at cryogenic temperatures. Here, we use a bespoke *in situ* test rig to show that helium ion irradiation produces a similar degradation in properties regardless of temperature, but room-temperature annealing leads to substantial recovery in the properties of cold-irradiated samples. We also report the first attempt at measuring the superconducting properties while the ion beam is incident on the sample, showing that the current that the superconductor can sustain is reduced by a factor of three when the beam is on.

Introduction

One option for the long-term decarbonization of electricity generation is to utilize the energy released when atoms with low binding energy fuse. Research into nuclear fusion reactors began in the 1950s and continues at an increasing pace in both private companies¹⁻⁴ and national and international laboratories.^{5,6} Current fusion reactor demonstrators, most of which are based on the tokamak concept,⁷ use strong magnetic fields to confine plasmas of deuterium and tritium. Because the physical space for magnet windings is often extremely limited, these magnets require conductors that can transport very high current densities (J_c), making superconducting materials the only

viable option. Coated conductors (CCs) made with a biaxially textured layer of the anisotropic high-temperature superconductor (HTS) REBa₂Cu₃O₇ (RE = rare-earth, REBCO) compounds are seen as a key-enabling technology for small fusion reactors,^{8,9} owing to their large engineering critical current densities (J_c) in high magnetic fields and at temperatures well above 4.2 K. However, in service, the electromagnets in a tokamak are exposed to fluxes of fast neutrons¹⁰ even with the addition of shielding materials,^{11,12} and it is known that the performance of superconducting materials degrades as a result of the damage created by neutron irradiation.¹³⁻¹⁵

Will Iliffe, Department of Materials, University of Oxford, Oxford, UK; Culham Centre for Fusion Energy, Abingdon, UK
 Kirk Adams, Department of Materials, University of Oxford, Oxford, UK
 Nianhua Peng, Surrey Ion Beam Centre, University of Surrey, Guildford, UK
 Greg Brittles, Tokamak Energy, Abingdon, UK
 Rod Bateman, Tokamak Energy, Abingdon, UK
 Aidan Reilly, Culham Centre for Fusion Energy, Abingdon, UK
 Chris Grovenor, Department of Materials, University of Oxford, Oxford, UK
 Susannah Speller, Department of Materials, University of Oxford, Oxford, UK; susannah.speller@materials.ox.ac.uk
 *Corresponding author
 doi:10.1557/s43577-022-00473-5



As with all Type II superconductors, the critical current density (J_c) of the REBCO layer in a CC is determined by the flux pinning landscape,^{*} produced in part by microstructural defects and is influenced by temperature (T), applied magnetic field vector (\mathbf{B}), and strain (ϵ). As irradiation with energetic particles modifies the defect landscape,^{16,17} J_c also evolves with fluence (ϕ)—number of incident particles per unit area—and depends on the particular type and energy of the irradiating particles. The resultant damage level in a given material is often reported in units of displacements per lattice atom (dpa), as this unit has been shown to correlate well with macroscopic changes in material properties.¹⁸

The extreme conditions experienced in the toroidal field (TF) magnet¹⁹ in a tokamak make this a particularly challenging application for REBCO CCs, especially because of the smaller scale of the latest generation of tokamak reactors (e.g., References 1, 4, 6). Designing these magnets for long-term operation will require detailed information on how the superconducting performance of REBCO CC at the operating temperature is influenced by simultaneous irradiation with both fusion spectrum neutrons and gamma rays, ideally with the superconductor carrying its full rated current and subject to high applied fields and strain. Given that no source of DT fusion neutrons of the appropriate fluence currently exists, experiments to determine $J_c(\mathbf{B}, T, \epsilon, \phi)$ values under true fusion conditions have not been possible. The majority of published experimental measurements have involved irradiating the CC samples at room temperature or above, followed by transferring them to a cryogenic measurement system to evaluate the effect of the irradiation on J_c as a function of temperature and applied magnetic field. Notable examples of this kind of *ex situ* experiment include exposure of CC to fission-spectrum neutrons by Fischer et al.^{14,20} and energetic ions (e.g., References 21, 22). These experiments all showed a systematic decrease in both critical temperature (T_c) and J_c in low field, accompanied by a decrease in anisotropy. However, in higher applied fields, J_c values initially increase with irradiation damage, before decreasing with further irradiation until eventually there is a complete loss of superconductivity. The fluence at which the peak in J_c occurs has been shown to be dependent on the sample temperature, the type of radiation, the direction of the applied field, and the nature of the original pinning landscape in the CC.²⁰ A more thorough description of these experiments can be found in Reference 23.

More recently, steps toward testing REBCO CC under fusion relevant conditions, such as cryogenic temperatures, have been undertaken. The first such experiment was reported by Sorbom²⁴ who used 1.2-MeV protons to irradiate YBCO CCs up to ≈ 0.003 dpa (3 mdpa) at 80 K, 323 K, and 423 K before allowing the samples to return to room temperature for an extended period prior to performing cryogenic transport

measurements. Sorbom's key conclusions were that irradiating REBCO at a lower temperature led to a slower decline in J_c value with increasing fluence. It was inferred from supporting molecular dynamics (MD) simulations that a higher proportion of the radiation-induced lattice defects formed at lower temperatures remained as isolated point defects because the slower diffusion kinetics restricted migration to and accumulation at the numerous low-angle grain boundaries present in these materials.²⁴ We have recently reported the first *in situ* J_c measurements on CC samples at 40 K in self-field, taken in between sequential irradiation doses with 2 MeV He⁺ ions without the samples being warmed to room temperature. By comparing the degradation in performance, when the samples were both irradiated and measured *in situ* at 40 K with samples irradiated at room temperature and then cooled for *ex situ* measurement,^{23,25} we showed that, although the J_c of both sets of samples seemed to degrade at approximately the same rate with increasing fluence, the J_c and T_c values of the cold-irradiated samples could be recovered to some extent after "annealing" at room temperature, whereas the superconducting properties of the room-temperature-irradiated samples declined slightly on further aging at room temperature. Most recently, Fischer et al. used proton irradiation at 77 K to investigate how annealing at 80–300 K affected the J_c and T_c values of damaged REBCO CC samples. Their results showed that there was no change in J_c values up to 110 K, suggesting that the irradiation-induced damage in REBCO is stable up to this temperature, but even short exposures to temperatures above 110 K led to improvements in both J_c and T_c values.²⁶ In light of these new *in situ* experiments, the apparent improvement in damage tolerance of CCs at low temperature reported in the original Sorbom study²⁴ can now be understood to result from the annealing out of some of the irradiation-induced defects during the room-temperature excursion before the superconducting properties were measured. The recovery of CC properties upon room-temperature annealing after cold irradiation and the importance of establishing whether the life of fusion magnets can be extended by annealing, led Unterrainer et al. to study the effects of annealing samples after neutron irradiation in a fission reactor. They found that both T_c and J_c values recovered on annealing at temperatures up to 200°C, with further property recovery at higher annealing temperatures when an oxygen atmosphere was used.²⁷ Even after this relatively small number of publications, it is already clear that irradiation with neutrons and ions creates lattice damage that results in a reduction in both the key superconducting parameters (T_c and J_c), and that the temperature history of the sample during and after irradiation is important in determining the superconducting properties and hence predicting the magnet performance under real service conditions.

The next step in emulating real operational conditions is to measure the superconducting properties while the lattice damage is being created (i.e., when neutrons or ion beam is interacting with the sample). Here, we report new experiments in which a GdBCO CC sample is cooled below T_c and then

* The size, shape, and distribution of defects relative to the characteristic penetration and coherence lengths of the superconducting material.⁴⁸



exposed to He⁺ ion irradiation while transporting a supercurrent. This has required a substantial redesign of our original experimental protocols. In addition, we have increased the number of cold and room-temperature-irradiated samples measured with the beam-off, added measurements taken after much shorter room-temperature anneals and explored the effect of a sequence of cold irradiation damage and room-temperature recovery cycles.

Experimental setup

The material used for this work was a GdBCO-based CC with a 2- μm -thick superconducting layer manufactured by Fujikura in 2018 using a combination of ion-beam-assisted deposition and pulsed laser deposition.^{28,29} Full details of the experimental setup are described in References 23 and 25. Briefly, in collaboration with the Surrey Ion Beam Centre (SIBC), an apparatus was built to measure the current–voltage (I – V) characteristics of 40–50- μm -wide tracks prepared in CCs using wet etching and photolithography while the sample is maintained at 40 K and exposed to irradiation damage by 2 MeV He⁺ ions. To minimize heating of the sample, transport measurements were taken using square current pulses of duration <0.12 s, with intervals between the pulses of >0.5 s. I – V curves were constructed by gradually increasing the amplitude of the current pulse and measuring the voltage during the duration of the pulse. The curves were fitted to a power law to determine I_c and n -values using

$$V = E_c L \left(\frac{I}{I_c} \right)^n,$$

where L is the track length and E_c is the electric field criterion. In line with other similar experiments (e.g., References 30, 31), a criterion of $E_c = 1 \mu\text{V cm}^{-1}$ was used to extract I_c values. Quenches that could damage the tracks were avoided by increasing the pulse amplitude by the smallest possible increment allowed by the power supply (0.02 A) and stopping the experiment when only a small voltage was measured across the superconducting track ($V \approx 30 \mu\text{V}$). Here, T_c is defined as the temperature where the resistance of the sample is 50% of that measured at 100 K and the transition width (ΔT_c) is defined as the temperature range over which the sample resistance changes from 10 to 90% of the 100 K resistance value. T_c measurements were performed with a constant current of ≈ 0.1 A ($J \approx 0.1 \text{ MA cm}^{-2}$).

Because this study is aimed at mimicking neutron damage in REBCO, analysis using the SPECTRA-PKA code^{32,33} was used to define suitable irradiation parameters for our sample based on the neutron irradiation experiments of Fischer et al.²⁰ In these experiments, a GdBCO CC was irradiated in the Central Irradiation Facility of the Vienna TRIGA reactor³⁴ with fission-spectrum neutrons up to a total fluence of $\approx 4 \times 10^{18} n_f \text{ cm}^{-2}$, where n_f is the number of fast neutrons (defined as neutrons with energy >0.1 MeV). This is equivalent to a damage level of 4.4 mdpa accumulated at a rate of $8.3 \times 10^{-9} \text{ dpa s}^{-1}$, and the SPECTRA-PKA calculation suggests that oxygen

primary knock-ons contribute the largest proportion (59.2%) of the total damage.²⁵ SRIM[†] analysis³⁵ was then used to define a suitable ion-energy combination that would allow us to excite the oxygen ions in the REBCO lattice. Selecting a dpa rate similar to that achieved in the TRIGA reactor would occupy the SIBC beam line for unacceptably long periods, so a rastered beam of 2 MeV He⁺ ions at a beam current density of 100 nA cm^{-2} was selected to provide a damage rate of $6.4 \times 10^{-7} \text{ dpa s}^{-1}$ (≈ 77 times faster than the TRIGA damage rate) and requiring a total cumulative irradiation duration of ≈ 130 min to reach damage levels similar to the maximum fluence reached by Fischer et al. (4.4 mdpa).²⁰

Following the method described by Unterrainer et al.,²⁷ a furnace annealing study on one of the cold-irradiated samples (C4) was performed in flowing oxygen in a tube furnace. The sample was heated at $20^\circ\text{C min}^{-1}$ to 150°C and held at this temperature for 24 h, after which the sample was allowed to cool naturally inside the furnace.

The samples reported in this work were tested under two distinct conditions, referred to as “beam-on” and “beam-off,” respectively. An additional protocol (see **Figure 1**) was developed for the beam-on experiments to protect the sample from thermal runaway in the event that the beam dramatically degraded the superconducting properties. The beam-on protocol involved increasing the magnitude of the current pulses in coarse steps (to minimize the time taken) to determine a rough beam-on I_c value at which the voltage exceeds the overvoltage limit (i.e., $V > 30 \mu\text{V}$). After a short delay of >60 s to allow the temperature equilibrium to reestablish, a series of repeated current pulses of constant magnitude below this initial beam-on I_c estimate were applied to the sample as irradiation progressed, and the stability of the voltage was monitored.

Results

Beam-off experiments

Details of the superconducting properties of all the samples discussed in this work, including those for the six samples reported in Reference 23, are shown in **Table I**. These show that $T_c > 90$ K—similar to the value determined using magnetometry—and $\Delta T_c < 2$ K for all samples except the anomalous sample RT2.[‡] Scanning electron microscopy (SEM) was used to determine the actual width of each track and confirms that the new samples reported in this work are free from cracks at the track edges that were commonly seen in the original samples reported in Reference 23 and can be attributed to extra care taken in the processing of the tracks (see Supplementary information Figure 1).

Figure 2 illustrates the change of T_c , ΔT_c and the critical current density normalized to the unirradiated value for each sample ($J_c/J_c(\text{initial})$) measured at 40 K as a result of He⁺ ion irradiation at room temperature (red) and *in situ* at 40 K

[†] For parameters, see footnote 5 of Reference 23.

[‡] Discussed in Reference 23.

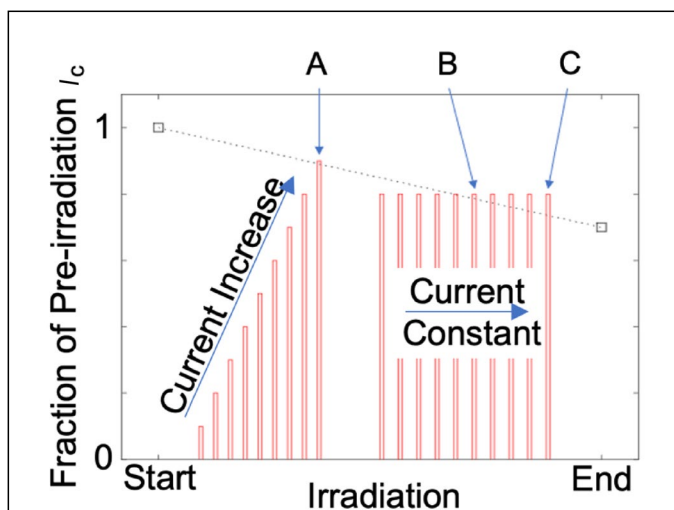


Figure 1. Schematic for beam-on testing protocol. The beam-off I_c is measured before and after ion irradiation (\square) and the dotted line illustrates an extrapolation of how the I_c value could decrease gradually under irradiation. During the irradiation period, the current pulses are applied to the sample in two stages. First, the current is increased in coarse steps until an overvoltage or quench response is detected (A). After a short delay to allow reestablishing of the temperature equilibrium, several current pulses of constant magnitude just under this peak current value are applied so that, as the sample I_c degrades under irradiation, an overvoltage will be measured when the applied current exceeds this gradually decreasing I_c value (B), eventually leading to the sample quenching (C).

(blue). All three of these superconducting parameters degrade systematically with increased damage level, with the cold-irradiated samples showing roughly the same damage rate as the room-temperature-irradiated samples. However, the samples that were irradiated cold show a significant increase in T_c and $J_c/J_c(\text{initial})$ and decrease in ΔT_c when allowed to anneal at room temperature for periods of ≈ 1 day and then more gradually for much longer periods, whereas the properties of the samples irradiated at room temperature do not change

significantly. This confirms our preliminary results reported in Reference 23 and strongly supports our original conclusion that sample RT2 was anomalous. The time-dependent recovery of superconducting properties on holding at room temperature after cold irradiation is illustrated for samples C4 and C5 in Figure 3. This shows that, for both samples, there is a rather rapid increase in the T_c and I_c values as a result of room-temperature annealing in the first 24 h for sample C5, but that the recovery continues more slowly over much longer periods ($\gtrsim 150$ days).

In addition, a cold-irradiated and room-temperature annealed sample (C4) has been subjected to a further cycle of *in situ* irradiation and room-temperature annealing (Figure 3a). To allow a direct comparison with the room-temperature annealing steps, the second cold irradiation experiment was stopped when the I_c value reached that obtained during the first cycle of cold irradiation of ≈ 0.71 A (equivalent to $J_c/J_c(\text{initial}) \approx 0.05$). The results shown in Figure 2 (and summarized in Supplementary information Table I) suggest that the J_c degradation in the second irradiation follows a similar trajectory as during the first cold irradiation, with T_c and ΔT_c returning to the same values that they had after the first cold irradiation. However, a key difference is that the rate of recovery of the superconducting properties after room-temperature annealing is substantially slower after the second cold irradiation step, despite them being damaged to the same T_c , ΔT_c and $J_c/J_c(\text{initial})$ values prior to annealing. However, the sample cold-irradiated twice does seem to eventually recover to a similar degree, with T_c and $I_c(40\text{ K})$ values increasing to $\approx 95\%$ and 80% of their pre-second cold irradiation values, respectively (although this conclusion is based on only one datapoint). Finally, C4 was subjected to a furnace anneal at 150°C in flowing oxygen for 24 h. This led to further recovery of T_c , ΔT_c , and I_c to values slightly higher than after the first room-temperature anneal, as shown in Figure 2 and Supplementary Table I.

Table I. Pristine sample properties.

Track	Measured Width (μm)	Length (mm)	T_c (K)	ΔT_c (K)	I_c (40 K) \pm 0.1	n (40 K) \pm 1	J_c (40 K) (MA/cm^2)
C1	36	4	90.8	0.7	5.1	21	7.1
C2	38	4	90.2	1.3	12.3	24	16.2
C3	46	2	90.3	0.9	14.2	26	15.4
C4	46	2	90.5	0.9	14.1 ^a	30 ^a	15.3 ^a
C5	48	2	91.0	1.3	15.8	26	16.5
RT1	34	4	90.2	0.9	9.2	23	13.5
RT2	37	4	89.6	1.6	7.2	21	9.7
RT3	40	2	90.8	1.2	8.9	30	11.1
RT4	49	2	90.7	1.7	12.2	25	12.7
RT5	54	2	90.5	0.9	15.0	27	13.9
RT6	42	2	90.6	1.2	14.3	17	17.0

^aOnly 1 I - V data set collected as sample quenched and post-quench the I_c had changed.

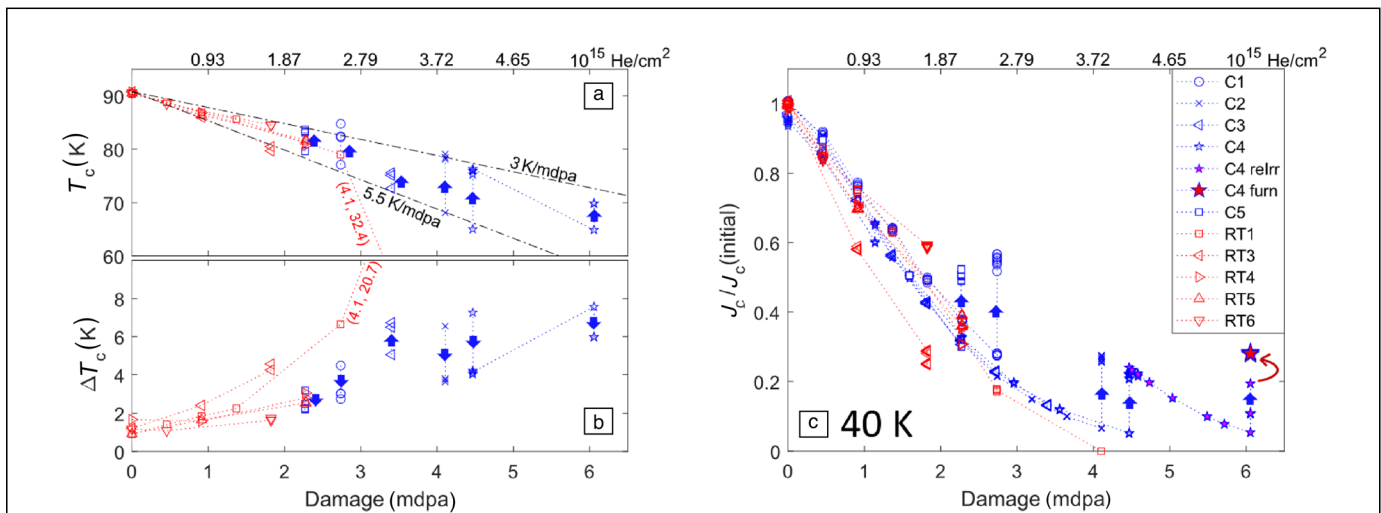


Figure 2. Evolution of the critical temperature T_c (a), the transition width ΔT_c (b), and the critical current density (J_c) (c) relative to its initial, unirradiated value [$J_c(\text{initial})$] at 40 K. Samples C1–5 were irradiated and measured *in situ* at 40 K without a warming step and samples RT1–6 were irradiated at room temperature and then cooled for measurement. Filled blue arrows indicate changes due to room-temperature annealing. The top axis shows the cumulative fluence of 2 MeV helium ions to the sample. Specific to sample C4 is “relrr,” which indicates data collected during and after a second cold irradiation step, and “furn,” which indicates data collected after furnace annealing at 150°C.

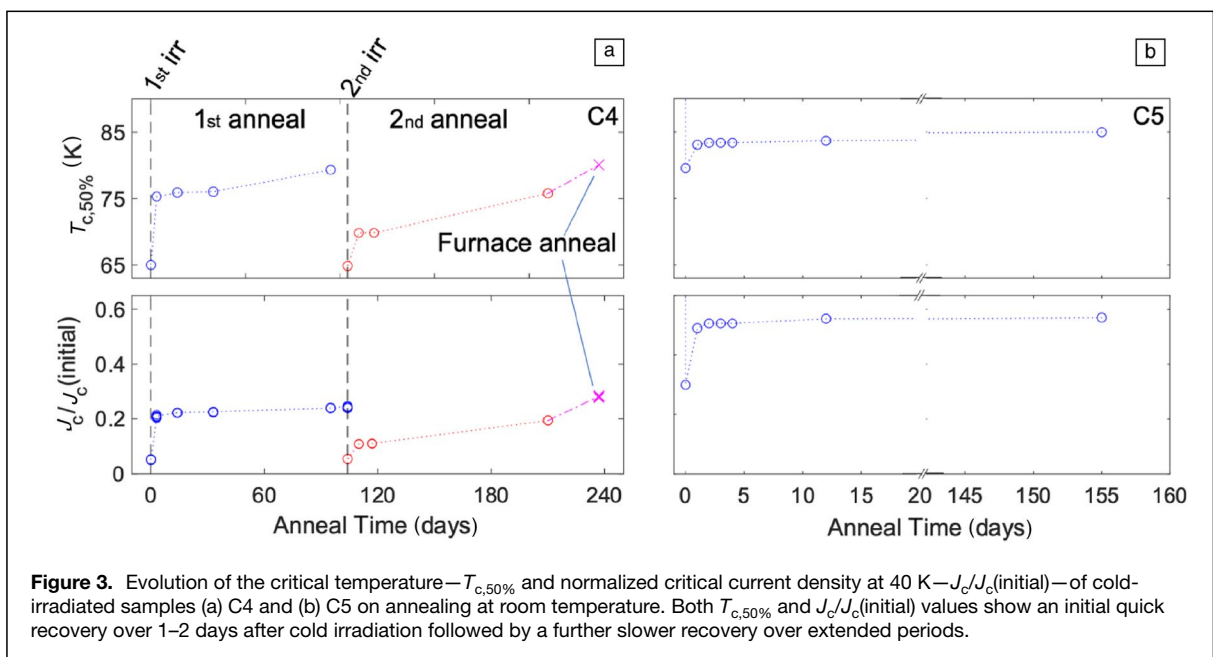
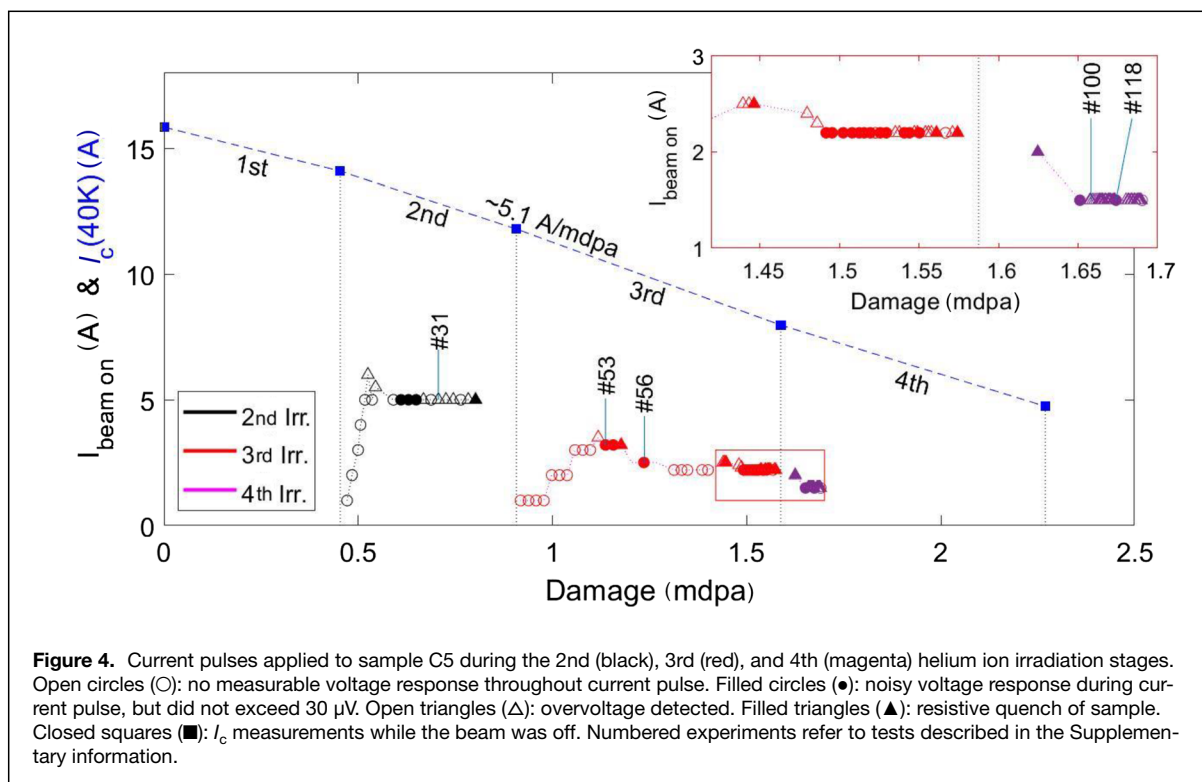


Figure 3. Evolution of the critical temperature— $T_{c,50\%}$ and normalized critical current density at 40 K— $J_c/J_c(\text{initial})$ —of cold-irradiated samples (a) C4 and (b) C5 on annealing at room temperature. Both $T_{c,50\%}$ and $J_c/J_c(\text{initial})$ values show an initial quick recovery over 1–2 days after cold irradiation followed by a further slower recovery over extended periods.

Beam-on experiments

Figure 4 shows the results of the beam-on experiments performed on sample C5 using the protocol shown in Figure 1. Beam-on tests were not performed during the first irradiation steps to ensure that this sample was reacting to the irradiation in a manner similar to previous *in situ*-irradiated samples, thus, minimizing the potential of blowing up the track. During the second irradiation step, the magnitude of the current pulse was increased to 6 A before an overvoltage ($>30 \mu\text{V}$) was detected. The current pulse amplitude was then reduced to 5 A and maintained at that level

for 13 consecutive 0.12 s pulses as the ion beam gradually added damage to the sample. Of these 13 pulses, three led to no measurable voltage response, three to a noisy voltage response ($<30 \mu\text{V}$), five to an overvoltage ($>30 \mu\text{V}$), and the final pulse led to a resistive quench ($\gg 30 \mu\text{V}$). A beam-off measurement was then performed, which confirmed that the sample had recovered from the quench, because the beam-off degradation of J_c followed the expected trend from the previous *in situ* beam-off measurements. Further beam-on measurements were performed during subsequent irradiation stages. The maximum current that could be



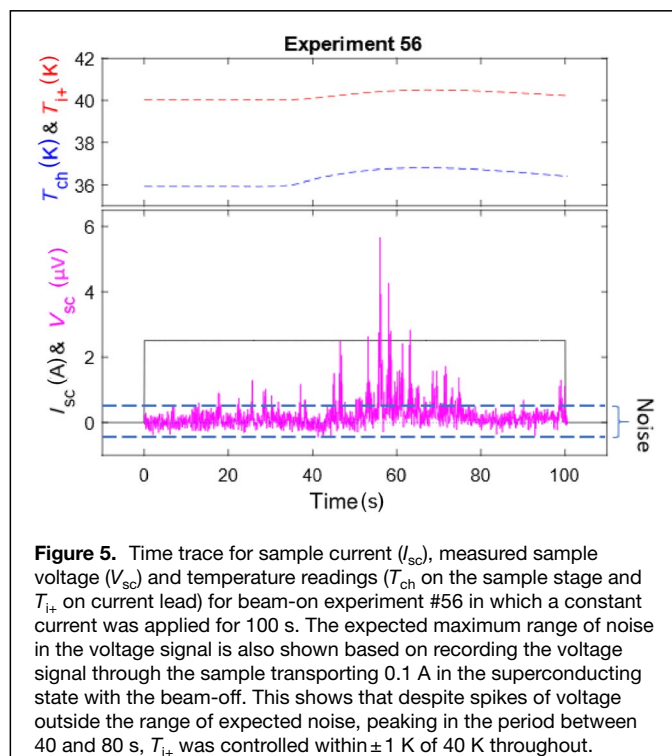
applied without a voltage being detected in the third irradiation stage was significantly lower than in the second irradiation stage (3 A compared to 5 A). Moreover, as the overall damage level increased during the third and fourth irradiation stages, pulses that led to voltage noise, overvoltages, and resistive quenches became more common, even though the applied current was reduced.

As we became more familiar with the behavior of the sample under ion-beam irradiation, test conditions such as the pulse length and measurement frequency were varied to further probe the sample performance. The results of a test of temperature and voltage stability under beam-on conditions—labeled #56 in Figure 4—are shown in Figure 5. This involved applying a 2.5 A, 100 s flat top pulse to the sample to assess whether the combination of rastering the beam and applying a continuous test current that was expected to elicit a voltage response affected the sample temperature and the nature of the voltage response. This test showed that the voltage across the superconductor was consistently noisy, but $<30 \mu$ V that the temperature of the sample did not rise significantly, and that the voltage response occasionally spiked during a period where current was applied for >500 times longer than the normal current pulse used in the rest of the experiments, and 50 times longer than the rastering cycle period of the ion beam.

Discussion

Beam-off experiments

The results of the beam-off experiments, summarized in Table I, show that both the tracks previously



reported (C1, C2, and RT1–4) and the new samples (C3–5 and RT5–6) have a spread of starting J_c values that can be attributed to local variations in microstructure of the CC. However, the initial T_c and ΔT_c values for all the samples are >89 K and <1.7 K, respectively, indicating that the REBCO layer is

not significantly damaged by the track fabrication process. Further to the results reported in Reference 23, the additional samples show a systematic decline in T_c at the rate of 5.5 K mdpa⁻¹ and $J_c/J_c(\text{initial})$ at 25–45% mdpa⁻¹ for both cold and room-temperature irradiation. This T_c decline rate is higher than the sample-independent rate reported by Fischer et al. for irradiation with fission-spectrum neutrons (2.4 K mdpa⁻¹,²⁰) and much higher than the 0.02–0.2 K mdpa⁻¹ range inferred from data reported by Haberkorn et al.,³⁶ Jiao et al.,³⁷ and Civale et al.³⁸ due to proton irradiation. The new *in situ* samples showed a similar recovery in properties to the previously reported samples on room-temperature annealing, with measurements taken after shorter annealing times for sample C5 (Figure 3b) suggesting a rapid initial recovery of the superconducting properties of these GdBCO tracks in the first days, followed by a gradual further recovery over much longer periods. Repeated *in situ* irradiation and room-temperature annealing of sample C4 (Figure 3a and in more detail in Supplementary Figure 3) show that the damage and recovery process can be reproduced on the same sample.

Fischer et al.²⁶ have shown similar recovery behavior at temperatures as low as 110 K in proton-irradiated REBCO, which suggests at least one recovery mechanism must have a low activation energy (E_a). Unterrainer et al.²⁷ have also explored recovery in neutron-irradiated samples at higher temperatures, showing that processes with much higher activation energies (only activated above 500 K) are also important in controlling T_c and J_c values if the loss of oxygen can be avoided. We have added our observation above that annealing a He⁺-irradiated sample in oxygen to 420 K for 24 h also recovers the J_c beyond the values achieved by long-term annealing at 300 K.

There seems, therefore, to be a general consensus that cold irradiation, by protons or He⁺ ions, leads to the creation of types of point defects that are different than those generated by room-temperature irradiation—some that have relatively high activation energies (E_a) for migration and, hence, remain essentially immobile at room temperature, but can be annealed out at higher temperatures, and others that have much lower activation energies and can be removed even at 110 K. Given that we would expect the concentrations of these defects to increase roughly linearly with irradiation fluence,^{18,39} there should be a systematic buildup of both immobile and mobile defect concentrations during irradiation at 40 K, followed in our annealing experiments (at 300 K and 450 K) by a decrease in the concentration of the defects that are mobile at each temperature. We illustrate in Figure 6 how a population of irradiation-induced defects with a distribution of E_a values could respond to annealing, and lead to a J_c performance similar to that we report in Figure 3. We are not able to propose the exact nature of the immobile and mobile defects, nor to speculate on what kind of defects are more detrimental to the superconducting properties, but note that Tolpygo et al.⁴⁰ conclude that

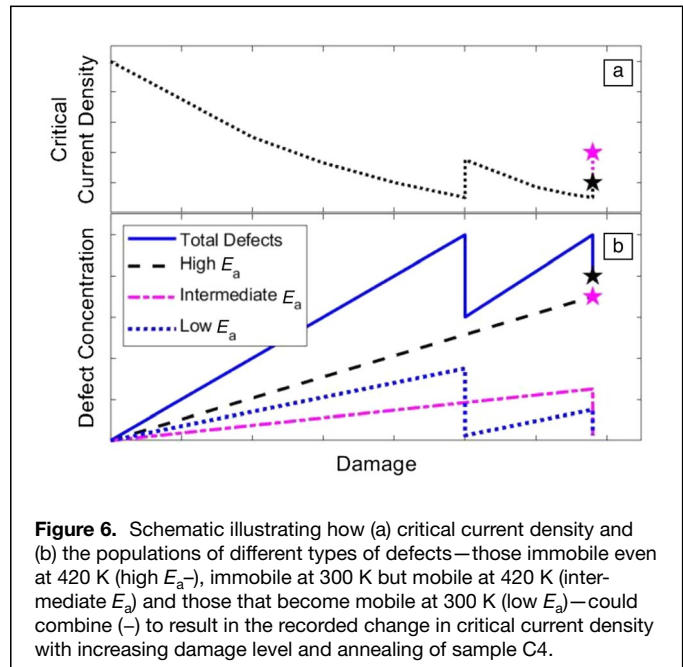


Figure 6. Schematic illustrating how (a) critical current density and (b) the populations of different types of defects—those immobile even at 420 K (high E_a), immobile at 300 K but mobile at 420 K (intermediate E_a) and those that become mobile at 300 K (low E_a)—could combine (–) to result in the recorded change in critical current density with increasing damage level and annealing of sample C4.

plane site defects are much more detrimental to T_c than chain site disorder, and that Gray et al.⁴¹ and others^{42–44} show that oxygen within REBCO is most easily displaced by irradiation because of its lower mass and relatively lower threshold displacement energy than the other ionic species in the REBCO lattice. To understand this in more detail, it will require investigation using experimental and modeling techniques that can identify the type of point defects generated under different damage conditions.

Because we are proposing that some of these specific defect populations can be reduced by annealing at room temperature, it is perhaps surprising that the rate of decline of $J_c/J_c(\text{initial})$ is similar for both *in situ* samples irradiated and measured at 40 K and *ex situ* samples irradiated at room temperature (Figure 2c). We speculate that this can be explained by dynamic annealing of the more mobile defects during room-temperature irradiation to effectively reduce the damage rate. This seems to be confirmed by the observation that there is no improvement in superconducting properties in the *ex situ* samples after further room-temperature annealing, noting that the time between irradiation and testing is typically several days. Therefore, we propose that the defect landscape created during irradiation is not the same at 300 K and 40 K, despite the apparent similarity in the rate of superconducting property degradation. It is possible during room-temperature irradiation that defects mobile at this temperature do not simply diffuse to sinks or mutually annihilate during irradiation, but they combine into more stable defect clusters that can only then be removed at higher annealing temperatures. Further investigation of the microstructural differences between *ex situ* irradiated and *in situ* post-annealed samples is, therefore, needed.



Beam-on experiments

The results from the beam-on experiments (Figure 4) indicate that the superconducting performance of the REBCO tracks is substantially degraded under ion irradiation, which suggests that direct interactions with the energetic ions may adversely affect the superconducting state. However, we must first consider the possibility that, owing to insufficient cooling power, direct heating by the ion beam is gradually raising the temperature inside the REBCO layer and consequently reducing I_c . Preliminary tests on sample C5 suggest that the sample temperature would need to increase from 40 to ≈ 65 K for the I_c to drop to $\approx 1/3$ of its beam-off value whereas temperature sensor data show deviations in temperature of less than ± 1 K during the ion irradiation of this sample (see Supplementary Figure 2). Even during the long pulse experiment, Figure 5 shows that application of the ion beam and a current of 2.5 A did not result in the temperature of the sample rising by >1 K, and the temperature control system acted sufficiently quickly to avoid any further temperature rise without reducing the heater output to zero. Although this gives us some confidence that there is no significant increase in temperature around the sample location during beam-on conditions, temperature increases in the narrow REBCO tracks cannot be completely ruled out as there is no temperature sensor in direct contact with the sample. However, a simple calculation based on modeling the REBCO layer as an isolated slab containing a random distribution of point heat sources with the surfaces of the slab held at a fixed temperature, the known flux of He⁺ ions, the energy deposited in the REBCO layer per ion from SRIM calculations and the film thickness suggest that the maximum temperature rise within the REBCO layer would be of the order of 10^{-4} K (for details, see Supplementary information). We, therefore, conclude that the temperature rise in the sample during beam-on experiments is negligible compared to that required to reduce sample I_c to $\approx 1/3$ of its beam-off value, and that it is some form of direct interaction with the ion beam that is affecting the superconducting properties of the track and reducing the current carrying capacity.

Energetic ions can interact and transfer energy to solid matter in two distinct processes: nuclear stopping and electronic stopping. In the nuclear stopping mechanism, energy is transferred from the incident ions to atoms in the material via elastic nuclear collisions. Provided the initial impact is sufficiently energetic, the target atom can be knocked out of its lattice site with enough energy to displace more atoms in the lattice, resulting in a small volume of material containing a concentration of point defects far above the equilibrium value.¹⁸ If enough of these defects are formed locally, they may be condensed into a collision cascade where the crystal structure is lost, but there is no evidence that He⁺ ions create this kind of gross damage.⁴⁵ The ballistic phase of the cascade, where atoms are being displaced, typically lasts for a fraction of a picosecond, and is followed by a slower relaxation process during which defects migrate and recombine, generally leaving some residual structural damage. MD simulations by Gray

et al.⁴¹ suggest that the defect structure in YBCO stabilizes within 1 ps, although any thermal effects are likely to take slightly longer to recover.⁴⁴ Presumably superconductivity would be disrupted locally within these regions, at least temporarily, even if there is minimal residual structural damage.

The electronic stopping mechanism involves charged incident beam ions undergoing a series of inelastic interactions with electrons, thereby losing energy gradually as they pass through the material. The subsequent thermalization of the highly excited electrons is expected to break numerous Cooper pairs, generating regions in the material where superconductivity is suppressed. If a transport current is present, it will redistribute to avoid these volumes, locally raising the current density. This mechanism is exploited in superconducting nanowire single photon detectors (SNSPDs)⁴⁶ where a transport current is chosen so that, when an electron is excited by an incoming photon, the local current density either exceeds J_c temporarily or superconductivity is sufficiently suppressed to allow vortex movement within the track, generating a spike in voltage that can be detected.⁴⁷

To assess which of these mechanisms is more likely to be responsible for the observed degradation in I_c value of the tracks, we have carried out some simple calculations based on the irradiation conditions of our experiment. Because He⁺ ions arriving at the REBCO surface are traveling at a velocity $v \approx 10^7$ m s⁻¹ and at a flux $J = 6.25 \times 10^{15}$ m⁻² s⁻¹, the volume of sample containing one ion is $\frac{v}{J} \approx 1.6 \times 10^{-9}$ m³. This is several orders of magnitude larger than the track volume (~ 2 m m $\times 50$ μ m $\times 2$ μ m = $2 \cdot 10^{-13}$ m³) so we can assume that ions are traveling through the film one by one, even though we are using relatively high ion fluxes to accelerate the damage rate. Based on the total energy deposited in the REBCO layer per ion (calculated by SRIM to be 4.8×10^5 eV) and the known flux of He⁺ ions, we find that an energy of approximately 0.5 eV per unit cell per second is deposited into the REBCO layer. Over the course of a 120 ms measurement pulse, this equates to 60 meV per unit cell per pulse. This is several orders of magnitude larger than the condensation energy of YBCO (≈ 0.2 meV) so it is reasonable to assume that there is sufficient energy deposited in the REBCO layer by electronic stopping of the He⁺ ions during the measurement current pulse to severely disrupt the superconducting state. Moreover, the SRIM results suggest that these electronic interactions account for 99.9% of the energy deposited directly in the REBCO layer, making this a much more likely candidate than nuclear interactions to explain the weakening of the superconducting state under irradiation with He⁺ ions.

Conclusions

Here, we report on further experiments investigating the recovery of the superconducting properties of biaxially textured GdBCO layers after 2 MeV He⁺ ion irradiation while the sample is maintained at 40 K, starting from both a pristine, unirradiated condition and after cold irradiation. Our results suggest that the defects created during cold irradiation have a range of activation energies, so that some can be annealed



out—leading to the recovery of the superconducting properties—at temperatures below 300 K for defects, others at 300–420 K, and a final group with higher activation energy that remains even after annealing at 420 K. This concept gives a clear focus for future modeling experiments to identify the nature of these defects so that the community can consider how to maximize the potential for recovery stages to reverse the degradation of superconducting properties after irradiation.

Using our new beam-on experimental protocol, we report that the voltage responses characteristic of the onset of instabilities and quenches are detected in CC tracks at much lower current densities during irradiation with 2 MeV He⁺ ions than the *I_c* values measured both before the ion beam is switched on and after it is turned off. After careful consideration of the possibility of this being a result of beam and/or ohmic heating effects, we conclude that this is a result of direct interactions between the energetic charged particle beam and the superconducting charge carriers. This interaction leads to a destabilization of the superconducting state, specifically by the release of energy from the ion beam to the REBCO layer by electronic stopping, and this results in the breaking of a large number of Cooper pairs per incident ion.

The in-service conditions of magnet components in a fusion machine will involve primary collisions with energetic neutrons rather than light ions, and in the absence of Coulombic interactions, we could expect no similar degradation effect. However, neutrons do generate both collision cascades and more widespread general lattice damage in REBCO,¹⁷ and so the primary knock-on ions generated from ballistic collisions with incident neutrons can then act like the He⁺ ions as the source of electronic stopping damage that will degrade the superconducting properties. The flux of neutrons in magnet components will be much lower than the accelerated conditions we have used here, but we note that each incident neutron will be able to generate thousands of primary and secondary knock-on ions.[§] We further suggest that the preliminary *in situ* experiments reported here indicate that the effect of irradiation damage on the performance of magnet windings will be impossible to avoid completely under fusion operation conditions, and so must be taken seriously in the design of superconducting electromagnets for fusion applications.

Funding

This work received support from the Engineering and Physical Sciences Research Council (Grant No. EP/W011743/1).

Data availability

The data sets generated and/or analyzed during the current study are available from the corresponding author on reasonable request.

[§] Based on a 70-keV oxygen PKA that was shown in Reference 25 to be the primary knock-on atom-energy combination, which was most prolific at generating lattice displacements in REBCO subject to 2 TF neutron spectra with vastly different neutron shielding philosophies.

Conflict of interest

On behalf of all authors, the corresponding author states that there is no conflict of interest.

Open access

This article is licensed under a Creative Commons Attribution 4.0 International License, which permits use, sharing, adaptation, distribution and reproduction in any medium or format, as long as you give appropriate credit to the original author(s) and the source, provide a link to the Creative Commons licence, and indicate if changes were made. The images or other third party material in this article are included in the article's Creative Commons licence, unless indicated otherwise in a credit line to the material. If material is not included in the article's Creative Commons licence and your intended use is not permitted by statutory regulation or exceeds the permitted use, you will need to obtain permission directly from the copyright holder. To view a copy of this licence, visit <http://creativecommons.org/licenses/by/4.0/>.

Supplementary information

The online version contains supplementary material available at <https://doi.org/10.1557/s43577-022-00473-5>.

References

1. Tokamak Energy (n.d.). <https://www.tokamakenergy.co.uk/>. Accessed 27 May 2022
2. S. Reed, "Nuclear Fusion Edges Toward the Mainstream," *New York Times* (October 18, 2021)
3. Commonwealth Fusion Systems (n.d.). <https://www.cfs.energy/>. Accessed 27 May 2022
4. B.N. Sorbom, J. Ball, T.R. Palmer, F.J. Mangiarotti, J.M. Sierchio, P. Bonoli, C. Kasten, D.A. Sutherland, H.S. Barnard, C.B. Haakonsen, J. Goh, C. Sung, D.G. Whyte, *Fusion Eng. Des.* **100**, 378 (2015). <https://doi.org/10.1016/j.fusengdes.2015.07.008>
5. M. Shimada, D.J. Campbell, V. Mukhovatov, M. Fujiwara, N. Kirneva, K. Lackner, M. Nagami, V.D. Pustovitov, N. Uckan, J. Wesley, N. Asakura, A.E. Costley, A.J.H. Donné, E.J. Doyle, A. Fasoli, C. Gormezano, Y. Gribov, O. Gruber, T.C. Hender, W. Houlberg, S. Ide, Y. Kamada, A. Leonard, B. Lipschultz, A. Loarte, K. Miyamoto, V. Mukhovatov, T.H. Osborne, A. Polevoi, A.C.C. Sips, *Nucl. Fusion* **47**(6), S1 (2007). <https://doi.org/10.1088/0029-5515/47/6/S01>
6. UK Atomic Energy Authority (UKAEA), Spherical Tokamak for Energy Production (n.d.). <https://step.ukaea.uk>. Accessed 27 May 2022
7. L.A. Artsimovich, *Nucl. Fusion* **12**, 215 (1972)
8. Y. Zhai, D. van der Laan, P. Connolly, C. Kessel, *Fusion Eng. Des.* **168**, 112611 (2021). <https://doi.org/10.1016/j.fusengdes.2021.112611>
9. F. Dahlgren, T. Brown, P. Heitzenroeder, L. Bromberg, *Fusion Eng. Des.* **80**(1–4), 139 (2006). <https://doi.org/10.1016/j.fusengdes.2005.06.357>
10. J. Freidberg, *Plasma Physics and Fusion Energy*, 1st edn. (Cambridge University Press, Cambridge, 2007)
11. A. Sykes, A.E. Costley, C.G. Windsor, O. Asunta, G. Brittles, P. Buxton, V. Chuyanov, J.W. Connor, M.P. Gryaznevich, B. Huang, J. Hugill, A. Kukushkin, D. Kingham, A.V. Langtry, S. McNamara, J.G. Morgan, P. Noonan, J.S.H. Ross, V. Shevchenko, R. Slade, G. Smith, *Nucl. Fusion* **58**(1), 016039 (2018). <https://doi.org/10.1088/1741-4326/aa8c8d>
12. M. Coleman, S. McIntosh, *Fusion Eng. Des.* **139**, 26 (2019). <https://doi.org/10.1016/j.fusengdes.2018.12.036>
13. M. Soell, C.A.M. van der Klein, H. Bauer Giesen, W.G.G. Vogl, *IEEE Trans. Magn.* **11**(2), 178 (1975)
14. R. Prokopec, D.X. Fischer, H.W. Weber, M. Eisterer, *Supercond. Sci. Technol.* **28**(1), 014005 (2015). <https://doi.org/10.1088/0953-2048/28/1/014005>
15. H.W. Weber, F. Nardai, C. Schwinghammer, R.K. Maix, *Neutron Irradiation of NbTi with Different Flux Pinning Structures, in Advances in Cryogenic Engineering Materials* (Springer, Boston, 1982), p. 329. https://doi.org/10.1007/978-1-4613-3542-9_32
16. K. Nordlund, S.J. Zinkle, A.E. Sand, F. Granberg, R.S. Averbach, R. Stoller, T. Suzudo, L. Malerba, F. Banhart, W.J. Weber, F. Willaime, S.L. Dudarev, D. Simeone, *Nat. Commun.* **9**, 1084 (2018). <https://doi.org/10.1038/s41467-018-03415-5>
17. Y. Linden, W.R. Iliffe, G. He, M. Danaie, D.X. Fischer, M. Eisterer, S.C. Speller, C.R.M. Grovenor, *J. Microsc.* **286**(1), 3 (2021). <https://doi.org/10.1111/jmi.13078>



18. G. Was, *Fundamentals of Radiation Materials Science*, 1st edn. (Springer, Berlin, 2007). <https://doi.org/10.1007/978-3-540-49472-0>
19. M.R. Gilbert, T. Eade, C. Bachmann, U. Fischer, N.P. Taylor, *Nucl. Fusion* **57**, 046015 (2017). <https://doi.org/10.1088/1741-4326/aa5bd7>
20. D.X. Fischer, R. Prokopec, J. Emhofer, M. Eisterer, *Supercond. Sci. Technol.* **31**(4), 044006 (2018). <https://doi.org/10.1088/1361-6668/aaadf2>
21. H. Matsui, T. Ootsuka, H. Ogiso, H. Yamasaki, M. Sohma, I. Yamaguchi, T. Kumagai, T. Manabe, *J. Appl. Phys.* **117**(4), 043911 (2015). <https://doi.org/10.1063/1.4906782>
22. N. Haberkorn, J. Guimpel, S. Suárez, J.-H. Lee, H. Lee, S.H. Moon, *Supercond. Sci. Technol.* **32**(12), 125015 (2019). <https://doi.org/10.1088/1361-6668/ab5164>
23. W. Iliffe, N. Peng, G. Brittles, R. Bateman, R. Webb, C. Grovenor, S. Speller, *Supercond. Sci. Technol.* **34**(9), 09LT01 (2021). <https://doi.org/10.1088/1361-6668/ac1523>
24. B.N. Sorbom, "The Effect of Irradiation Temperature on REBCO Jc Degradation and Implications for Fusion Magnets," PhD thesis, Massachusetts Institute of Technology, Cambridge (2017). <https://dspace.mit.edu/handle/1721.1/120392?show=full>. Accessed 30 May 2022
25. W. Iliffe, "Radiation Damage of Superconducting Materials for Fusion Application," DPhil thesis, University of Oxford, Oxford (2022). <https://ora.ox.ac.uk/objects/uuid:bab009f2-2b1d-42d7-a53c-bf914a128d7a>. Accessed 30 May 2022
26. D. Fischer, "Degradation and Annealing of Coated Conductors after Cryogenic Irradiation," presented at the 15th European Conference on Applied Superconductivity (EUCAS 2021), Moscow, September 5–9, 2021
27. R. Unterrainer, D.X. Fischer, A. Lorenz, M. Eisterer, *Supercond. Sci. Technol.* **35**(4), 04LT01 (2022). <https://doi.org/10.1088/1361-6668/ac4636>
28. Fujikura Europe Ltd., Fujikura HTS (n.d.). https://www.fujikura.co.uk/products/FEL2GHTS_High-Temperature-Superconductors
29. S. Fujita, S. Muto, W. Hirata, T. Yoshida, K. Kakimoto, Y. Iijima, M. Daibo, T. Kiss, T. Okada, S. Awaji, *IEEE Trans. Appl. Supercond.* **29**(5), 1 (2019). <https://doi.org/10.1109/TASC.2019.2896535>
30. S.C. Wimbush, N.M. Strickland, *IEEE Trans. Appl. Supercond.* **27**(4), 1 (2017). <https://doi.org/10.1109/TASC.2016.2628700>
31. N.M. Strickland, C. Hoffmann, S.C. Wimbush, *Rev. Sci. Instrum.* **85**, 113907 (2014). <https://doi.org/10.1063/1.4902139>
32. M.R. Gilbert, J.C. Sublet, *J. Nucl. Mater.* **504**, 101 (2018). <https://doi.org/10.1016/j.jnucmat.2018.03.032>
33. M.R. Gilbert, J. Marian, J.C. Sublet, *J. Nucl. Mater.* **467**, 121 (2015). <https://doi.org/10.1016/j.jnucmat.2015.09.023>
34. H.W. Weber, H. Bock, E. Unfried, L.R. Greenwood, *J. Nucl. Mater.* **137**, 236 (1986)
35. J.F. Ziegler, J.P. Biersack, M.D. Ziegler, *SRIM-Stopping Range of Ions in Matter*, 5th edn. (SRIM, Morrisville, 2015)
36. N. Haberkorn, J. Kim, S. Suárez, J.-H. Lee, S.H. Moon, *Supercond. Sci. Technol.* **28**(12), 125007 (2015). <https://doi.org/10.1088/0953-2048/28/12/125007>
37. Y. Chen, F. Yan, C. You, G. Zhao, Y. Jiao, *J. Alloys Compd.* **576**, 265 (2013). <https://doi.org/10.1016/j.jallcom.2013.04.160>
38. L. Civale, A.D. Marwick, M.W. McElfresh, T.K. Worthington, A.P. Malozemoff, F.H. Holtzberg, J.R. Thompson, M.A. Kirk, *Phys. Rev. Lett.* **65**(9), 1164 (1990)
39. M.T. Robinson, *J. Nucl. Mater.* **216**, 1 (1994). [https://doi.org/10.1016/0022-3115\(94\)90003-5](https://doi.org/10.1016/0022-3115(94)90003-5)
40. S.K. Tolpygo, J.-Y. Lin, M. Gurvitch, S.Y. Hou, J.M. Phillips, *Phys. Rev. B* **53**(18), 462 (1996)
41. R.L. Gray, M.J.D. Rushton, S.T. Murphy, *Supercond. Sci. Technol.* **35**(3), 035010 (2022). <https://doi.org/10.1088/1361-6668/ac47dc>
42. F. Cui, H. Li, L. Jin, Y. Li, *Nucl. Inst. Methods Phys. Res. B* **91**, 374 (1994)
43. F.Z. Cui, J. Xie, H.D. Li, *Phys. Rev. B* **46**(17), 182 (1992)
44. Av. Krashenninnikov, K. Nordlund, *J. Appl. Phys.* **107**(7), 071301 (2010). <https://doi.org/10.1063/1.3318261>
45. R.W. Harrison, N. Peng, R.P. Webb, J.A. Hinks, S.E. Donnelly, *Fusion Eng. Des.* **138**, 210 (2019). <https://doi.org/10.1016/j.fusengdes.2018.11.024>
46. L. You, *Nanophotonics* **9**(9), 2673 (2020). <https://doi.org/10.1515/nanoph-2020-0186>
47. A. Engel, J.J. Renema, K. Il'in, A. Semenov, *Supercond. Sci. Technol.* **28**(11), 114003 (2015). <https://doi.org/10.1088/0953-2048/28/11/114003>
48. T. Matsushita, *Flux Pinning in Superconductors*, 2nd edn. (Springer, Cham, 2016) □

Publisher's note Springer Nature remains neutral with regard to jurisdictional claims in published maps and institutional affiliations.